Available online at ScienceDirect

Nuclear Engineering and Technology

journal homepage: www.elsevier.com/locate/net

NUCLEAR ENGINEERING AND TECHNOLOGY

Original Article

Physics Study of Canada Deuterium Uranium Lattice with Coolant Void Reactivity Analysis

Jinsu Park [a], *Hyunsuk Lee* [a], *Taewoo Tak* [a], *Ho Cheol Shin* [b], and *Deokjung Lee* [a,*]

[a] *Ulsan National Institute of Science and Technology, 50, UNIST-gil, Ulsan, 44919, Republic of Korea*
[b] *Korea Hydro and Nuclear Power Central Research Institute (KHNP-CRI), 70, Yuseong-daero 1312beon-gil, Yuseong-gu, Daejeon, 34101, Republic of Korea*

ARTICLE INFO

Article history:
Received 18 February 2016
Received in revised form
24 May 2016
Accepted 1 July 2016
Available online 29 July 2016

Keywords:
Advanced Canada Deuterium Uranium Reactor-700
Canada Deuterium Uranium-6
Coolant Void Reactivity
Sensitivity Study
Single Bundle and Checkerboard Voiding

ABSTRACT

This study presents a coolant void reactivity analysis of Canada Deuterium Uranium (CANDU)-6 and Advanced Canada Deuterium Uranium Reactor-700 (ACR-700) fuel lattices using a Monte Carlo code. The reactivity changes when the coolant was voided were assessed in terms of the contributions of four factors and spectrum shifts. In the case of single bundle coolant voiding, the contribution of each of the four factors in the ACR-700 lattice is large in magnitude with opposite signs, and their summation becomes a negative reactivity effect in contrast to that of the CANDU-6 lattice. Unlike the coolant voiding in a single fuel bundle, the 2×2 checkerboard coolant voiding in the ACR-700 lattice shows a positive reactivity effect. The neutron current between the no-void and voided bundles, and the four factors of each bundle were analyzed to figure out the mechanism of the positive coolant void reactivity of the checkerboard voiding case. Through a sensitivity study of fuel enrichment, type of burnable absorber, and moderator to fuel volume ratio, a design strategy for the CANDU reactor was suggested in order to achieve a negative coolant void reactivity even for the checkerboard voiding case.

1. Introduction

The Canada Deuterium Uranium (CANDU) reactor has been widely used in many countries because of its advantages such as its low absorption cross section of heavy water and inexpensive fuel manufacturing cost [1]. The Advanced CANDU Reactor-700 (ACR-700) was proposed by Atomic Energy of Canada Limited (AECL) as a next-generation CANDU reactor [2]. The main changes of ACR-700 are reducing the fuel pitch, changing the coolant material from heavy water to light water, and changing the 37-element CANDU-6 fuel bundle to a 43-element CANFLEX fuel bundle, which is an advanced fuel bundle design developed by AECL along with Korean Atomic Energy Research Institute for use in CANDU design nuclear reactors [3]. The CANFLEX fuel bundle contains slightly enriched uranium in the outer rods and natural uranium with burnable poison in the central rod. The most significant improvement is that the lattice of ACR-700 has a negative coolant void reactivity (CVR), unlike the previous CANDU lattice.

Models of the CANDU-6 and ACR-700 fuel lattices were constructed for a single bundle to understand the physics related to CVR. However, the fuel channels were connected in a CANDU

* *Corresponding author.*
E-mail address: deokjung@unist.ac.kr (D. Lee).
http://dx.doi.org/10.1016/j.net.2016.07.003

core with two independent pressure heads in a checkerboard pattern. In addition, the coolants of adjacent channels flowed in opposite directions. Therefore, in the case of a pressure pump failure in a loss-of-coolant accident, the coolant within a CANDU core does not void uniformly in 1–2 seconds, owing to the remaining pressure head. In other words, there may be coolant void bundles adjacent to normal fuel bundles in a checkerboard pattern during an accident situation. In this study, a coolant void analysis of the ACR-700 fuel lattice is expanded to a checkerboard case to describe the real operation conditions.

In order to understand the physics issues related to the CVR of a CANDU reactor, a familiar four-factor formula was used to predict the specific contributions to reactivity changes [4–6]. The situation of coolant voiding should bring about a change of neutron behavior, so the neutron spectral changes and neutron current were also analyzed. The models of the CANDU-6 and ACR-700 fuel lattices were constructed using the Monte Carlo code MCNP6, and its neutronic analyses were performed with the F tally capability in MCNP6 [7]. ACR-700 was improved from the CANDU reactor by changing the fuel enrichment and the moderator to fuel volume ratio (fuel pitch), and by inserting a burnable neutron absorber in the central pin of the fuel lattice. The CANDU fuel lattice, which shows better behavior in terms of CVR, can be searched through sensitivity studies of each design parameter, such as fuel enrichment, fuel pitch, and types of burnable absorbers.

Section 2 describes the models of the CANDU-6 and ACR-700 fuel lattices in terms of configurations, materials, and temperature data, and also presents the CVR analysis of single fuel bundles based on the four-factor formula and neutron spectrum. Section 3 presents the CVR analysis of checkerboard voiding. Section 4 provides the optimized CANDU fuel bundle in terms of CVR through the sensitivity study of fuel enrichment, moderator to fuel volume ratio, and burnable absorber of the ACR-700 fuel bundle.

2. CVR analysis of single fuel bundle

CVR analysis was performed on two-dimensional CANDU-6 and ACR-700 fuel lattices with a reflective boundary condition. Models of a single fuel bundle were constructed by MCNP6 using the ENDF/B-VII.0 continuous energy cross section library based on the specification from Atomic Energy of Canada Limited. The Monte Carlo simulation parameters were set to 500,000 histories per cycle with 400 active cycles and 100 inactive cycles, in order to keep the standard deviation of the multiplication factor smaller than 5 pcm. The four factors were calculated from the fission and absorption reaction rates, and they were computed using the F4 tally capability of MCNP6. The simulation was carried out for 0% voiding and instantaneous 100% voiding of the coolant.

2.1. *Description of fuel lattice*

There are 37 fuel elements of natural uranium in a CANDU-6 fuel bundle, and the material of coolant and moderator is heavy water. The lattice pitch of a CANDU-6 fuel bundle is 28.6 cm, and the moderator to fuel volume ratio is 16.4. The 43-element CANFLEX fuel bundle of ACR-700 contains natural uranium with a burnable poison in the center rod and slightly enriched uranium in the outer rods. The lattice pitch of a CANFLEX fuel bundle is 22.0 cm, and the moderator to fuel volume ratio is 7.1. The coolant material of ACR-700 has been changed from heavy water to light water. Fig. 1 illustrates the radial configurations of the two fuel lattices. Table 1 presents the model parameters of the CANDU-6 and ACR-700 fuel lattices for the simulations reported in this paper, such as material, density, geometrical, and temperature data. The figures of the fuel lattices were made using MCNPX visual editor [8].

2.2. *Normalized neutron spectra*

Fig. 2 shows the normalized neutron spectra of a CANDU-6 fuel lattice at 0% and 100% coolant voiding. Since most neutron moderations occur within the sufficiently big moderator region of the calandria of the CANDU-6 reactor, the coolant voiding does not affect the amount of overall neutron moderation. However, the up-scattering effect, caused by the collisions of neutrons from the low-temperature moderator region with the high-temperature coolant molecules, decreases because of the reduction of the coolant density, and it

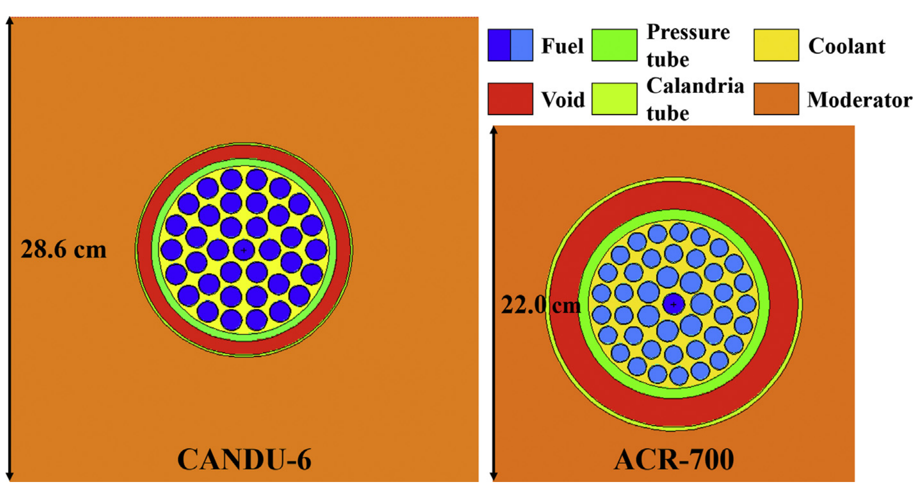

Fig. 1 – Radial configurations of CANDU-6 and ACR-700 fuel lattices.

Table 1 – Model description of CANDU-6 and ACR-700 fuel lattices.

	Material	Density (g/cm^3)	Outer radius (cm)	Temperature (K)
CANDU-6				
Fuel	0.72 wt% UO_2	10.65	0.614	1,010.16
Cladding	Zircaloy-4	6.550	0.654	1,010.16
Coolant	D_2O	0.797	5.170	573.16
Pressure tube	Zircaloy-2	6.550	5.620	573.16
Void	He	0.0014	6.460	–
Calandria tube	Zircaloy-2	6.550	6.600	353.16
Moderator	D_2O	1.080	–	353.16
ACR-700				
Inner fuel	0.72 wt% UO_2	10.65	0.629	1,010.16
Outer fuel	2.10 wt% UO_2	10.65	0.533	1,010.16
Cladding	Zircaloy-4	6.550	0.675/0.575	1,010.16
Coolant	H_2O	0.722	5.170	573.16
Pressure tube	Zr–2.5% Nb	6.570	5.819	573.16
Void	He	0.0014	7.550	–
Calandria tube	Zr alloy	6.440	7.800	353.16
Moderator	D_2O	1.080	–	353.16

results in a thermal spectrum shift to a lower energy region. In addition, the loss of coolant causes the reduction of high-energy neutron moderation in the fuel lattice and results in hardening of the high-energy spectrum. The coolant voiding of a CANDU-6 fuel lattice results in energy shifts for both the thermal and the fast parts of the neutron energy spectrum. After the coolant voiding, the thermal energy spectrum slightly shifts to a lower energy range, which has a larger fission cross section of ^{235}U and causes an increase in thermal fission. The fast spectrum shift to a harder energy range also causes an increase of fast fission of ^{238}U. Therefore, the reactivity effect of voiding is positive in the CANDU-6 lattice.

Fig. 3 illustrates the normalized neutron spectra of an ACR-700 fuel lattice at 0% and 100% coolant voiding. In contrast to the spectral change of the CANDU-6 fuel lattice, there is a significant reduction of thermal flux on coolant voiding. The reduction of fuel lattice pitch and the increment of the slowing-down power of light water compared with that of heavy water lead to more neutron moderations in the coolant of the ACR-700 than in the CANDU-6 fuel lattice. Therefore, the reduction of thermal neutrons results in a negative reactivity change in the case of coolant voiding.

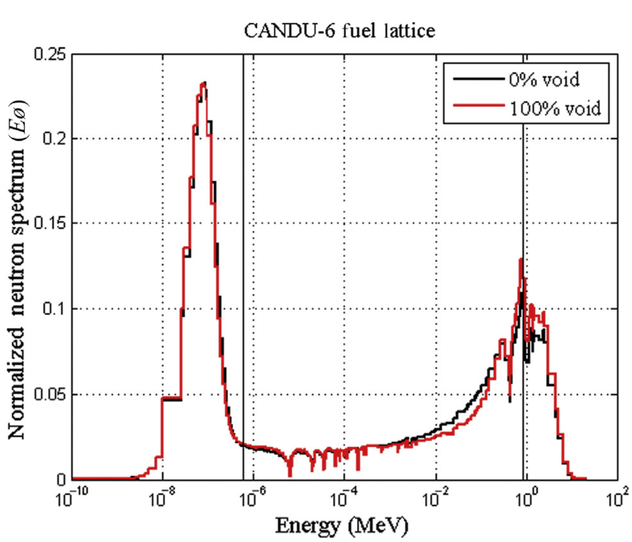

Fig. 2 – Neutron spectra of CANDU-6 fuel lattice at 0% and 100% coolant void.

2.3. *Four-factor analysis of void reactivity components*

CVR is the difference in reactivities before and after coolant voiding. The reaction rates were calculated with the three-group energy structure: thermal (0–0.625 eV), epithermal (from 0.625 eV to 0.821 MeV), and fast (0.821–20 MeV). The resonance escape probability is separated into epithermal and fast groups to clearly understand the physics of coolant voiding. The four factors include the fast fission factor (ε), resonance escape probabilities (p_E and p_F), thermal utilization factor (f), and reproduction factor (η_T). Table 2 summarizes the specific contribution of each parameter to the total reactivity

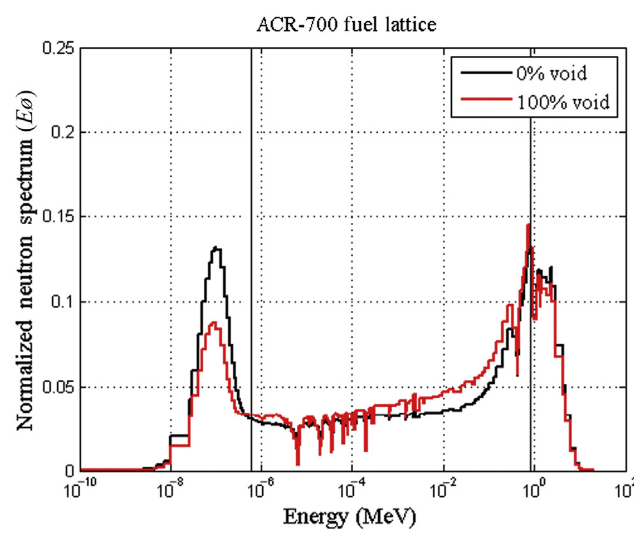

Fig. 3 – Neutron spectra of ACR-700 fuel lattice at 0% and 100% coolant void.

Table 2 – Void reactivity components of ACR-700 and CANDU-6 lattices.

	Factor	Coolant 0% void	Coolant 100% void	Reactivity effect (mk)	
CANDU-6	ε	1.08392	1.08953	$\Delta\rho_\varepsilon$	4
	p_E	0.85544	0.86476	$\Delta\rho_{p_E}$	9
	p_F	0.97593	0.97317	$\Delta\rho_{p_F}$	−2
	f	0.95028	0.95299	$\Delta\rho_f$	3
	η_T	1.32060	1.32220	$\Delta\rho_{\eta_T}$	1
	k_∞	1.13561	1.15534	CVR	15
ACR-700	ε	1.14305	1.20110	$\Delta\rho_\varepsilon$	37
	p_E	0.74989	0.68563	$\Delta\rho_{p_E}$	−68
	p_F	0.97508	0.97056	$\Delta\rho_{p_F}$	−4
	f	0.91288	0.95990	$\Delta\rho_f$	39
	η_T	1.65115	1.62647	$\Delta\rho_{\eta_T}$	−12
	k_∞	1.25980	1.24786	CVR	−8

change for the two fuel lattices. The differences between the CVR components in this study and previous work [5,6] are caused by the differences of simulation codes and neutron cross section libraries adopted. Through the work in this research, the results of CVR analysis for CANDU are updated with the latest neutronic simulation code.

Reactivity contributions of each factor in the CANDU-6 fuel lattice are relatively small in magnitude, and the summation of all components becomes positive. The fast fission factor provides a positive reactivity contribution in the CANDU-6 fuel lattice because of the hardened spectrum in the fission spectrum energy range. The epithermal resonance escape probability also provides a positive reactivity contribution because of the redistribution of epithermal neutrons to the moderator region, thereby reducing the ^{238}U resonance absorption. The reduction of thermal neutron absorption by the coolant provides a positive effect on the thermal utilization factor, and the shift in the thermal spectrum to a range with a larger thermal fission cross section and a smaller macroscopic capture cross section results in the reproduction factor providing a positive reactivity contribution. By contrast, the fast resonance escape probability provides a negative contribution because the fast neutron shifts to the higher energy level and the down-scattering ability is decreased.

In contrast to the CANDU-6 lattice, the reactivity contributions of each factor in the ACR-700 lattice are large in magnitude, and the summation of all components becomes negative. The fast fission factor provides a positive reactivity contribution due to spectrum hardening. As the reduction of moderator to fuel volume ratio leads to insufficient neutron moderation in coolant voiding, the reactivity contribution is much larger in magnitude than that in the CANDU-6 lattice. The impact on the epithermal resonance escape probability is large and negative because of the reduced moderation in coolant voiding. Similar to the CANDU-6 lattice, the fast resonance escape probability provides a negative reactivity contribution. The thermal utilization factor provides a much larger positive contribution in the ACR-700 lattice than in CANDU-6 because the voiding of light water decreases neutron absorption in the coolant more than that of heavy water. The reduction of thermal flux and thermal fission results in the reproduction factor making a negative reactivity contribution.

3. CVR analysis of checkerboard voiding

As previously stated, it can be inferred that the ACR-700 lattice can be safer than the CANDU-6 lattice in accident situations such as coolant boiling because the ACR-700 lattice has a negative CVR. However, it should be noted that the coolant pumping system of a CANDU reactor operates like a checkerboard. In other words, the flows of coolant between adjacent fuel bundles are in opposite directions. Therefore, the accident situation of a single pump failure can cause checkerboard voiding in the ACR-700 lattice, instead of full voiding in the previous section.

3.1. *Description of checkerboard model*

Fig. 4 illustrates the radial configuration of the checkerboard coolant voiding situation of an ACR-700 fuel lattice. The two-dimensional ACR-700 fuel lattice model was constructed to simulate the checkerboard coolant voiding. Each bundle was modeled as one-fourth of a bundle with symmetry in the center plane and with reflective boundary conditions. The geometry and material specifications of checkerboard voiding are the same as those of the ACR-700 single fuel lattice. Three-group neutron currents are calculated at the surface between the coolant 0% void bundle and 100% void bundle. The reaction rates for obtaining the four factors are also calculated for the coolant 0% void bundle and 100% void bundle.

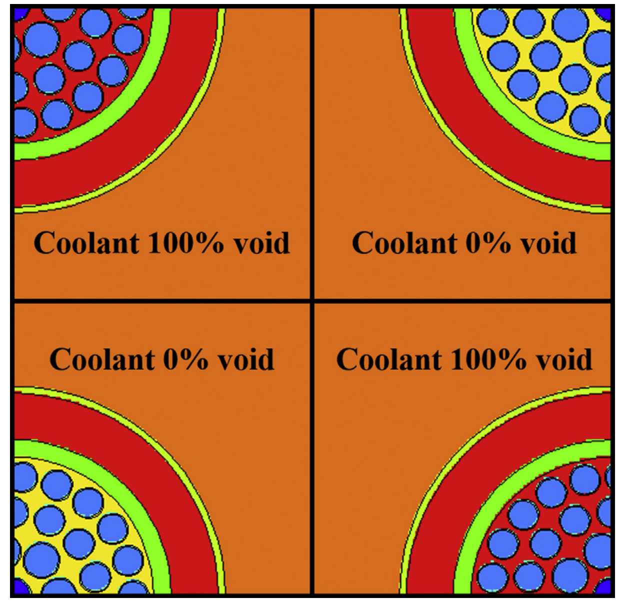

Fig. 4 – Radial configuration of checkerboard voiding of ACR-700 lattices.

3.2. *Spectral and three-group neutron current analyses*

Fig. 5 shows the spectrum changes of the center pin in no-void and 100% void channels in checkerboard voiding. The plots are normalized to a single fission source neutron in the 2 × 2 checkerboard. It can be noted that the voided channel has higher fluxes than the no-void channel in both high and low energy ranges due to decreased neutron absorption by the loss of coolant in the voided channel. The voided channel shows a harder spectrum at high energy than the no-void channel, and a softer spectrum at low energy, which will be explained by the three-group current analysis below. The no-void channel also has slightly higher fluxes than the normal bundle due to the inflow of neutrons from the voided channel.

Table 3 presents the three energy group surface currents normalized per fission source neutron of the 0% void ACR-700 bundle at normal and checkerboard coolant voiding conditions. It is noted that most neutron currents at surfaces consist of thermal and epithermal energy neutrons. As the ACR-700 lattice has a smaller moderator to fuel volume ratio than CANDU-6, fast neutrons are moderated insufficiently in the coolant voiding bundle. This results in an increase in the amount of fast and epithermal neutrons moving from the

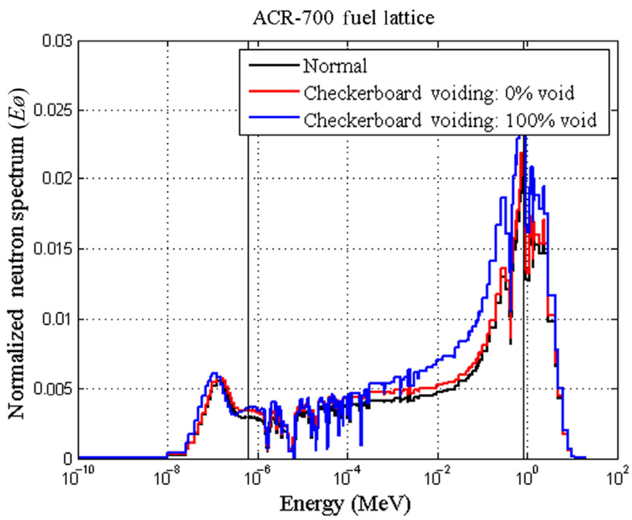

Fig. 5 – Spectrum changes of ACR-700 center rod in checkerboard voiding.

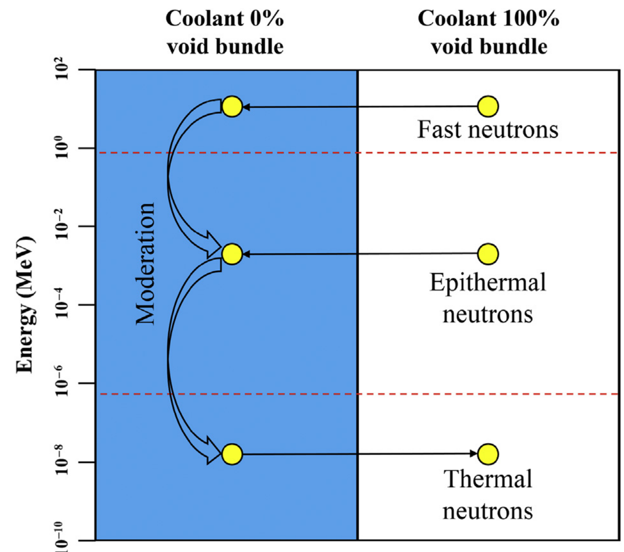

Fig. 6 – Neutron behavior in checkerboard coolant voiding.

100% void to no-void channels and also in a reduction of the amount of thermal neutron current leaving the voided channel. Therefore, it increases the fast fission of ^{238}U in the voided channel, and at the same time, the thermal fission reaction at the 100% void bundle increases due to the increase in thermal neutrons from the 0% void bundle to the 100% void bundle. Overall, the checkerboard coolant voiding in the ACR-700 fuel lattice results in more fission reactions, which leads to a positive reactivity effect. Fig. 6 illustrates the neutron behaviors when checkerboard coolant voiding occurs. Fast and epithermal group neutrons in the 100% voided bundle move to the no-void bundle and are moderated to the thermal group in that channel. The thermal neutrons then come back to the voided channel. This new path for neutron moderation in checkerboard voiding is the main reason for a positive CVR, whereas it is negative in full voiding.

3.3. *Four-factor analysis of checkerboard coolant voiding*

Table 4 presents the void reactivity components of an ACR-700 fuel lattice in normal and checkerboard coolant voiding conditions. By comparing the variations of the specific contributions from single bundle voiding in Table 2 and checkerboard voiding in Table 4, it should be noted that the epithermal resonance escape probability and the reproduction factor have a significant role in making a positive CVR in checkerboard coolant voiding, in contrast to single bundle voiding. As fast neutrons can be moderated in the 0% voided bundle in checkerboard voiding, the increment of epithermal and fast fluxes is smaller than that in single bundle coolant voiding. By reducing the resonance absorption, as the spectrum shifts to a range of smaller absorption cross sections, the epithermal resonance escape probability contributes less to reactivity in checkerboard voiding than to single bundle voiding. The reproduction factor also contributes less to reactivity in checkerboard voiding than that in single bundle voiding because the decrement of the thermal fission reaction rate in checkerboard voiding is smaller than that in single bundle voiding. Unlike the epithermal resonance escape probability and the reproduction factor, the fast fission factor, fast resonance escape probability, and thermal utilization factor make more negative reactivity contributions to checkerboard coolant voiding than to single bundle full voiding. As there is an additional path for moderation with checkerboard voiding, more fast neutrons can be moderated than in single bundle voiding, and as a result the fast fission factor contribute a smaller positive reactivity change. Contribution of the thermal utilization factor is positive as the fuel and moderator absorption reaction also decreases in checkerboard voiding. However, because the decrement of the moderator absorption reaction rate in checkerboard voiding is much smaller than that in single bundle voiding, the thermal utilization factor makes a smaller contribution to positive reactivity. In conclusion, checkerboard coolant voiding leads to a positive reactivity effect in contrast to single bundle coolant voiding.

Table 3 – Surface currents from no-void channel of ACR-700 fuel lattice on normal and checkerboard voiding.

	Normal condition (#/cm^2)	Checkerboard voiding (#/cm^2)		
		Incoming	Outgoing	Net
Fast	4.546E−02	5.305E−02	4.846E−02	−4.591E−03[a]
Epithermal	4.162E−01	5.068E−01	4.924E−01	−1.442E−02[a]
Thermal	4.875E−01	4.537E−01	4.691E−01	1.542E−02[a]

[a] A positive sign means a neutron flow from no-void to voided channel, and a negative sign means a neutron flow from voided to no-void channel.

Table 4 – Void reactivity components of ACR-700 lattice in normal and checkerboard voiding conditions.

Factor	Normal condition	Checkerboard voiding			Reactivity effect (mk)	
		Coolant 0% void	Coolant 100% void	Total		
ε	1.14305	1.15946	1.16977	1.16454	$\Delta\rho_\varepsilon$	14
p_E	0.74989	0.70832	0.73973	0.72375	$\Delta\rho_{p_E}$	−27
p_F	0.97508	0.97376	0.96680	0.96950	$\Delta\rho_{p_F}$	−5
f	0.91288	0.91533	0.95961	0.93656	$\Delta\rho_f$	20
η_T	1.65115	1.64528	1.65355	1.64934	$\Delta\rho_{\eta_T}$	−1
k_∞	1.25980	1.20437	1.32746	1.26223	CVR	1.52

4. Sensitivity study of ACR-700 fuel lattice

As stated in previous sections, while the ACR-700 fuel lattice has a negative CVR in the case of single bundle coolant voiding, it has a positive CVR in checkerboard voiding. In order to make the CVR negative, even with checkerboard voiding, a CVR analysis was performed for design parameters such as fuel enrichment, lattice pitches, and types of burnable absorbers. A sensitivity study of enrichment was performed for the outer fuel rods, with enrichments of 0.72%, 2.10%, and 4.50%. Besides dysprosium, several burnable absorber materials, such as erbia (Er_2O_3), gadolinia (Gd_2O_3), and boron carbide (B_4C), were tested for checkerboard voiding. Appendix 1 presents the detailed results of the sensitivity study on moderator to fuel volume ratio, fuel enrichment, and types of burnable absorbers for the CANDU-6 and ACR-700 fuel lattices.

4.1. *Sensitivity study of fuel enrichment and moderator to fuel volume ratio*

Fig. 7 shows the multiplication factors of the CANDU-6 and ACR-700 lattices as functions of the moderator to fuel volume ratio at hot zero power conditions. The yellow points represent the current CANDU-6 and ACR-700 fuel lattices. The black tangential lines on those yellow points represent the rate of reactivity changes due to variations of the moderator to fuel volume ratio, i.e., the steeper the slopes, the bigger the reactivity changes. It is apparent from the figure that the ACR-700 lattice is further undermoderated than CANDU-6, which makes the ACR-700 CVR negative in the full voiding case.

Fig. 8 shows the multiplication factor versus moderator to fuel volume ratio behaviors of the ACR-700 fuel lattices with 0.72 wt%, 2.10 wt%, and 4.50 wt% ^{235}U-enriched UO_2 fuels. Yellow points in the figure represent the current cases with a lattice pitch of 22.0 cm. It should be noted that the slopes of tangential lines at those yellow points are bigger for higher enrichment. In other words, higher enrichment of fuel makes the lattice more undermoderated at the same moderator to fuel volume ratio.

Fig. 9 shows the CVR versus moderator to fuel volume ratio behaviors of single bundle coolant voiding and checkerboard voiding for various ^{235}U enrichments. The yellow points in the figure represent the current ACR-700 lattice design. With current geometries, fuel lattices with 4.50 wt% enriched fuel have negative CVRs on both single bundle voiding and checkerboard voiding, and lower enrichment lattices show positive CVRs. It is apparent that either the increase of enrichment or the decrease of moderator to fuel volume ratio can reduce the CVR.

4.2. *Sensitivity study of burnable neutron absorber*

There is a burnable neutron absorber (7.5 wt% dysprosium) in the center fuel rod of the ACR-700 bundle to help the CVR become negative. A sensitivity study of the burnable absorber was carried out for different burnable absorber materials that have been used in Pressurized Water Reactors (PWRs) [9]. Gadolinia has been used in most PWRs due to the high

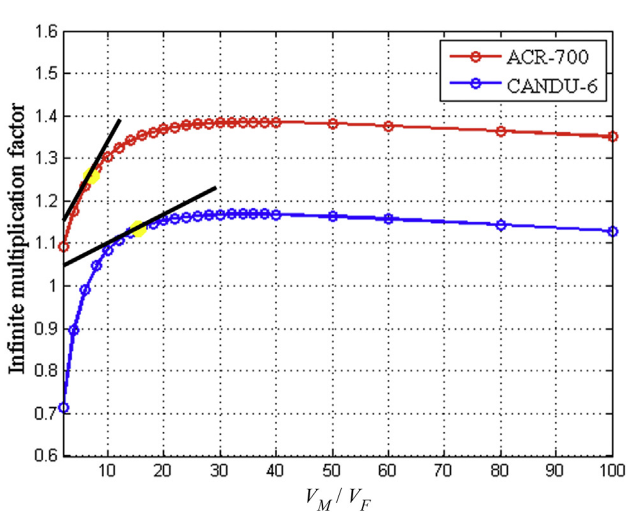

Fig. 7 – Multiplication factor as a function of moderator to fuel volume ratio.

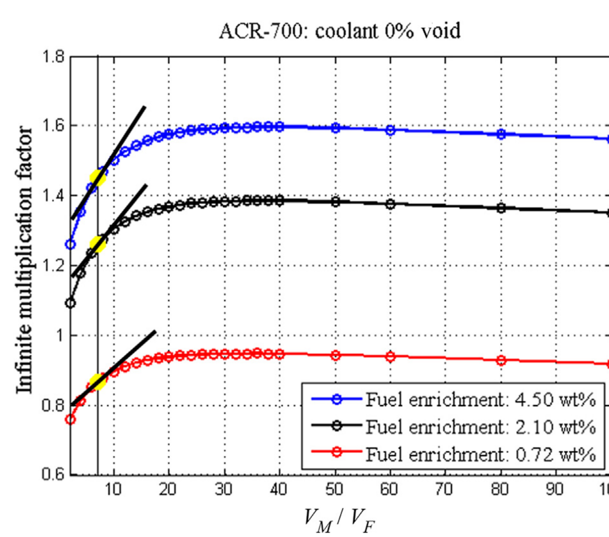

Fig. 8 – Multiplication factor behaviors for various enrichments of ^{235}U.

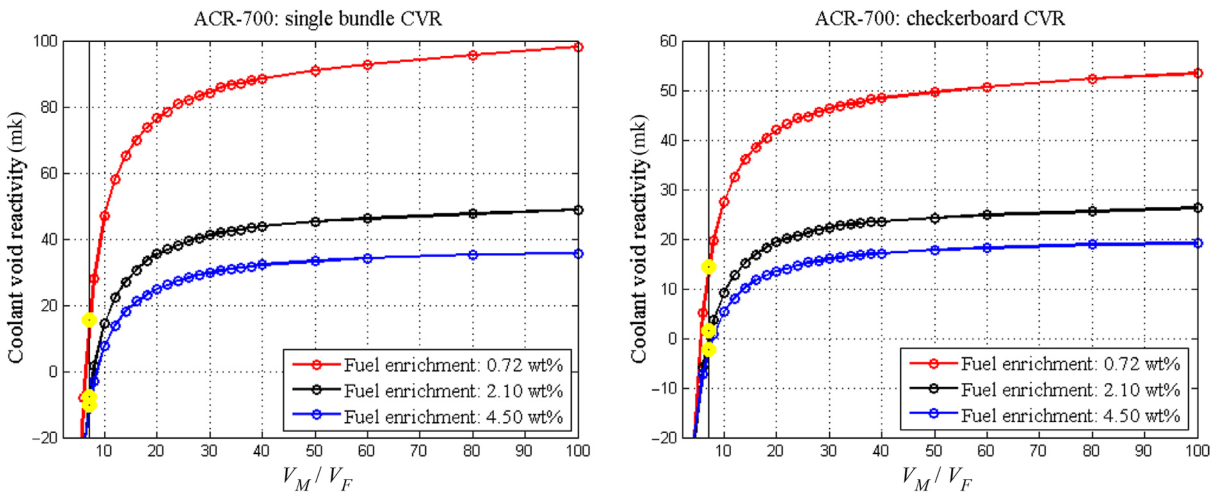

Fig. 9 – CVR for variations of ^{235}U enrichment in single bundle voiding and checkerboard coolant voiding.

absorption cross section of gadolinium. Erbia is also used in PWRs because ^{167}Er has a unique thermal absorption resonance that results in improved control of moderator temperature coefficient. Boron carbide is presently one of the most widely used absorbing materials for control rods owing to its high neutron absorption capability, high melting point, very low radioactive waste, and ease of reprocessing, and the low cost of natural B_4C. The simulation was performed by replacing dysprosium with different burnable absorber materials mixed into UO_2.

Fig. 10 shows the multiplication factor behaviors of fuel bundles with four burnable absorber materials. The yellow points in the figure indicate the points with the weight percent of each burnable absorber, which can make the initial excess reactivity the same as that using 7.5 wt% dysprosium. Note that boron carbide can achieve the same initial excess reactivity with the smallest weight percent of burnable absorber.

Fig. 11 shows the CVR behaviors depending on burnable absorbers in single fuel bundle and checkerboard coolant voiding conditions. When the weight percentages of burnable absorbers are chosen such that the initial reactivities are the same as those using 7.5 wt% dysprosium, the fuel bundles with gadolinia, erbia, or boron carbide have negative CVRs with single bundle coolant voiding, but positive CVRs with checkerboard coolant voiding. It was found that the ACR-700 fuel bundle with boron carbide as the burnable absorber instead of dysprosium had a slightly negative CVR even with checkerboard voiding.

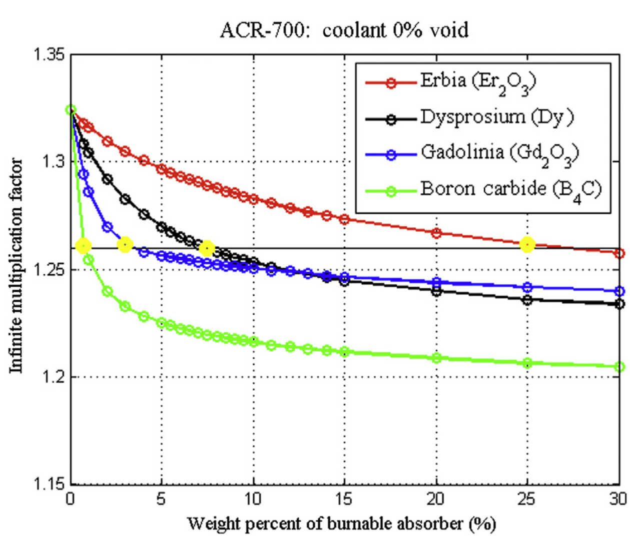

Fig. 10 – Multiplication factor using various types of burnable absorbers.

5. Conclusion

The CVR analyses of the CANDU-6 and ACR-700 fuel lattices were performed in single bundle coolant voiding and checkerboard voiding. The underlying physics of the CVR was explained by analyzing the spectral shifts and four-factor reactivity contributions. Upon single fuel bundle coolant voiding, the ACR-700 lattice has a negative CVR in contrast to the CANDU-6 lattice, because the ACR-700 lattice is undermoderated. Unlike single channel coolant voiding, the ACR-700 bundle has a positive reactivity change upon 2×2 checkerboard coolant voiding. This is because the epithermal resonance escape probability and the reproduction factor provide smaller contributions to reactivity from reducing the resonance absorption, as the spectrum shifts to a range of smaller absorption cross sections and a smaller decrement of thermal fission reaction rate, with checkerboard voiding than with single bundle voiding. It was noted that neutrons from the voided channel move to the no-void channel, where they lose energy and come back to the voided channel as thermal neutrons. This phenomenon causes a positive CVR when checkerboard voiding occurs. A sensitivity study revealed the effects of the moderator to fuel volume ratio, fuel enrichment, and burnable absorber on the CVR. A fuel bundle with a low moderator to fuel volume ratio and high fuel enrichment can help achieve a negative CVR. Additionally, it was found that boron carbide, instead of dysprosium, can result in the fuel bundle having a negative CVR, even with checkerboard coolant voiding.

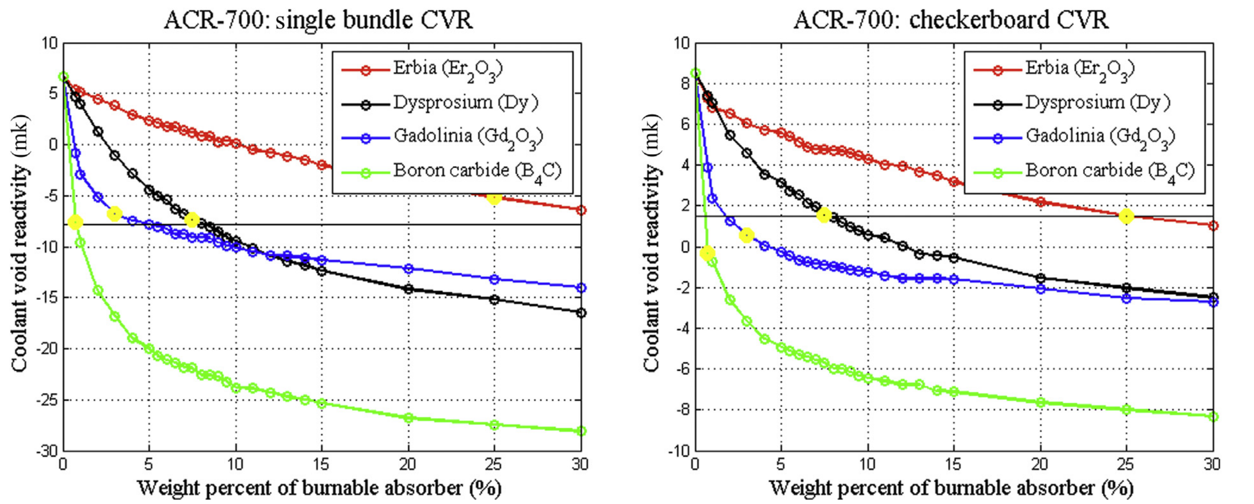

Fig. 11 – CVR behaviors depending on burnable absorber materials in single bundle voiding and checkerboard coolant voiding.

Conflicts of interest

The authors declare no conflict of interest.

Acknowledgments

This work was supported by the National Research Foundation of Korea (NRF) grant funded by the Korean Government (MSIP; NRF-2014M2A8A1032045).

Appendix 1

In Section 4.1, the sensitivity study on moderator to fuel volume ratio and fuel enrichment was explained. The single bundle and checkerboard coolant void models of the CANDU-6 and ACR-700 lattices were simulated with various moderator to fuel volume ratios by changing the fuel pitch. Table A1 lists the multiplication factors of the CANDU-6 and ACR-700 fuel lattices with various moderator to fuel volume ratios.

Table A1. Multiplication factors of CANDU-6 and ACR-700 lattices for sensitivity study about moderator to fuel volume ratio.

V_M/V_F	CANDU-6			ACR-700		
	Pitch (cm)	k_∞	STD[a] (pcm)	Pitch (cm)	k_∞	STD[a] (pcm)
2	14.9830	0.71476	2	16.5377	1.09229	2
4	17.6673	0.89740	2	18.8642	1.17687	2
6	19.9944	0.99238	2	20.9337	1.23545	2
7.1117	–			22.0000	1.25984	2
8	22.0776	1.04838	2	22.8162	1.27610	2
10	23.9805	1.08437	2	24.5549	1.30518	2
12	25.7431	1.10868	2	26.1783	1.32605	2
14	27.3925	1.12608	2	27.7068	1.34169	2
14.2875	28.5750	1.13561	2	–		
16	28.9481	1.13830	2	29.1552	1.35335	2
18	30.4243	1.14750	2	30.5350	1.36158	2
20	31.8321	1.15410	2	31.8551	1.36819	2
22	33.1802	1.15909	2	33.1227	1.37352	2
24	34.4756	1.16238	2	34.3435	1.37763	2
26	35.7241	1.16498	2	35.5223	1.37995	2
28	36.9304	1.16675	2	36.6633	1.38209	2
30	38.0985	1.16795	2	37.7698	1.38350	2
32	39.2319	1.16851	2	38.8448	1.38409	2
34	40.3334	1.16878	2	39.8909	1.38474	2
36	41.4056	1.16863	2	40.9102	1.38513	2
38	42.4508	1.16856	2	41.9047	1.38481	2
40	43.4708	1.16786	2	42.8762	1.38504	2
50	48.2486	1.16325	2	47.4360	1.38171	2
60	52.5941	1.15722	2	51.5944	1.37636	2
80	60.3538	1.14339	2	59.0389	1.36415	2
100	67.2236	1.12916	2	65.6446	1.35081	2

[a] STD, Standard deviation of multiplication factor.

The sensitivity study on fuel enrichment of the ACR-700 lattice was performed by changing the enrichment of ^{235}U in the outer three rings of fuel elements from 2.10 wt% to 0.72 wt% and 4.50 wt%. Table A2 lists the CVR results of the single bundle and checkerboard models of the ACR-700 lattice with various ^{235}U enrichments of the outer three rings of fuel elements.

In Section 4.2, the sensitivity study on the burnable absorber for the ACR-700 fuel lattice was performed to investigate the effects of the burnable absorber on the CVR. Originally, the central fuel pin in the ACR-700 lattice contains the 7.5 wt% dysprosium in natural uranium as burnable absorber. The sensitivity study was performed by mixing other burnable absorbers such as erbia, gadolinia, and boron carbide in natural uranium instead of dysprosium. The ACR-700 lattice was simulated with various weight percentages of burnable absorbers, and the multiplication factor results are listed in Table A3.

Table A2. CVR of ACR-700 lattice for sensitivity study of moderator to fuel volume ratio and ^{235}U enrichment.

ACR-700		0.72 wt%		2.10 wt%		4.50 wt%	
V_M/V_F	Pitch (cm)	Single bundle CVR (mk)	Checkerboard CVR (mk)	Single bundle CVR (mk)	Checkerboard CVR (mk)	Single bundle CVR (mk)	Checkerboard CVR (mk)
2	16.538	−420.4	−95.14	−289.7	−73.47	−208.4	−57.92
4	18.864	−99.05	−23.80	−84.84	−25.92	−69.25	−22.81
6	20.934	−7.981	5.174	−23.77	−5.747	−23.48	−7.207
7.1117	22.816	15.55	14.44	−7.840	1.523	−10.34	−2.157
8	24.555	28.07	19.56	1.453	3.765	−3.006	0.866
10	26.178	47.08	27.40	14.46	9.187	7.623	5.308
12	27.707	57.90	32.49	22.18	12.70	13.89	8.045
14	29.155	65.06	36.18	26.99	15.11	18.06	10.10
16	30.535	69.92	38.40	30.52	16.85	21.10	11.74
18	31.855	73.59	40.42	33.45	18.30	23.20	12.73
20	33.123	76.49	41.94	35.48	19.46	24.86	13.45
22	34.343	78.49	43.12	36.89	20.04	26.21	14.03
24	35.522	80.95	44.33	38.07	20.62	27.36	14.73
26	36.663	81.97	44.71	39.36	21.29	28.33	15.26
28	37.770	83.36	45.66	40.24	21.85	29.18	15.59
30	38.845	84.28	46.24	41.15	22.18	29.74	16.02
32	39.891	85.82	46.90	41.95	22.77	30.46	16.30
34	40.910	86.65	47.21	42.46	22.92	30.98	16.63
36	41.905	87.02	47.42	42.82	23.10	31.26	16.76
38	42.876	87.89	48.10	43.52	23.52	31.75	16.97
40	47.436	88.50	48.38	43.75	23.54	32.17	17.09
50	51.594	90.91	49.58	45.19	24.21	33.29	17.78
60	59.039	92.83	50.61	46.24	24.78	34.19	18.13
80	65.645	95.57	52.37	47.58	25.50	35.20	18.84
100	16.538	98.10	53.42	48.92	26.26	35.66	19.07

Table A3. Multiplication factors of ACR-700 lattice for sensitivity study on types of burnable absorbers.

Burnable absorber (wt%)	Dysprosium		Erbia		Gadolinia		Boron carbide	
	k_∞	STD[a] (pcm)	k_∞	STD[a] (pcm)	k_∞	STD[a] (pcm)	k_∞	STD[a] (pcm)
0.00	1.32426	2	1.32426	2	1.32426	2	1.32426	2
0.75	1.30851	2	1.31780	2	1.27387	2	1.26052	2
1.00	1.30455	2	1.31592	2	1.27120	2	1.25414	2
2.00	1.29201	2	1.30943	2	1.26461	2	1.23954	2
3.00	1.28259	2	1.30439	2	1.26095	2	1.23259	2
4.00	1.27560	2	1.30035	2	1.25812	2	1.22835	2
5.00	1.26997	2	1.29666	2	1.25621	2	1.22523	2
5.50	1.26750	2	1.29462	2	1.25548	2	1.22384	2
6.00	1.26493	2	1.29318	2	1.25481	2	1.22245	2
6.50	1.26331	2	1.29160	2	1.25424	2	1.22149	2
7.00	1.26147	2	1.29036	2	1.25339	2	1.22070	2
7.50	1.25984	2	1.28860	2	1.25282	2	1.21949	2
8.00	1.25825	2	1.28747	2	1.25215	2	1.21892	2
8.50	1.25684	2	1.28597	2	1.25144	2	1.21798	2

Table A3 – (*continued*)

Burnable absorber (wt%)	Dysprosium		Erbia		Gadolinia		Boron carbide	
	k_∞	STD[a] (pcm)	k_∞	STD[a] (pcm)	k_∞	STD[a] (pcm)	k_∞	STD[a] (pcm)
9.00	1.25544	2	1.28512	2	1.25120	2	1.21732	2
9.50	1.25473	2	1.28373	2	1.25082	2	1.21669	2
10.00	1.25335	2	1.28254	2	1.25050	2	1.21629	2
11.00	1.25111	2	1.28055	2	1.24928	2	1.21466	2
12.00	1.24924	2	1.27826	2	1.24886	2	1.21385	2
13.00	1.24793	2	1.27654	2	1.24798	2	1.21302	2
14.00	1.24619	2	1.27495	2	1.24677	2	1.21227	2
15.00	1.24492	2	1.27336	2	1.24643	2	1.21157	2
20.00	1.23996	2	1.26668	2	1.24364	2	1.20868	2
25.00	1.23602	2	1.26155	2	1.24177	2	1.20636	2
30.00	1.23392	2	1.25734	2	1.24002	2	1.20484	2

[a] STD, Standard deviation of multiplication factor.

The specific amounts of burnable absorbers in the central pin of the ACR-700 lattice were determined by making the initial reactivity the same as that with 7.5wt% dysprosium. After that, the single bundle and checkerboard models were simulated; the CVR results are listed in Table A4.

Table A4. CVR results of the single bundle and checkerboard models of the ACR-700 lattice with various types of burnable absorbers.

Burnable absorber (wt%)	Dysprosium		Erbia		Gadolinia		Boron carbide	
	Single bundle CVR (mk)	Checkerboard CVR (mk)	Single bundle CVR (mk)	Checkerboard CVR (mk)	Single bundle CVR (mk)	Checkerboard CVR (mk)	Single bundle CVR (mk)	Checkerboard CVR (mk)
0.00	6.6712	8.5326	6.6712	8.5326	6.6712	8.5326	8.5326	6.6712
0.75	4.6742	7.3826	5.3462	7.2798	−0.8480	3.8714	−0.3083	−7.5484
1.00	3.9528	7.0466	5.1621	6.8105	−2.8722	2.3514	−0.7509	−9.5805
2.00	1.2563	5.4444	4.4761	6.5455	−5.1144	1.2543	−2.5856	−14.2941
3.00	−1.0534	4.5641	3.8130	6.0294	−6.8329	0.5566	−3.6563	−16.8164
4.00	−2.8567	3.5494	2.8928	5.7290	−7.4675	0.0442	−4.5319	−18.9624
5.00	−4.3969	3.1398	2.3422	5.5603	−7.8004	−0.2345	−4.9392	−20.0380
5.50	−5.0380	2.7301	2.1479	5.3916	−8.0165	−0.4570	−5.1164	−20.7084
6.00	−5.4133	2.5673	1.7243	5.1322	−8.3039	−0.6738	−5.2937	−21.0587
6.50	−6.2923	2.1627	1.7285	4.8666	−8.8245	−0.7591	−5.3836	−21.3603
7.00	−6.7772	1.9439	1.3550	4.7929	−8.7324	−0.8300	−5.5356	−21.8691
7.50	−7.8397	1.5232	1.2026	4.7530	−9.1117	−0.9009	−5.6875	−21.9273
8.00	−7.8742	1.4317	0.8738	4.7131	−9.0955	−0.9718	−5.9933	−22.6013
8.50	−8.0597	1.1761	0.7913	4.6822	−9.1581	−1.0427	−5.9889	−22.5798
9.00	−8.5702	0.9771	0.2482	4.5674	−9.5932	−1.1136	−6.1324	−22.7471
9.50	−9.1321	0.7781	0.4064	4.4527	−9.9199	−1.1845	−6.3239	−23.2779
10.00	−9.4391	0.5790	0.1276	4.2806	−10.1152	−1.2554	−6.4379	−23.8012
11.00	−10.1542	0.4279	−0.5248	4.0163	−10.4707	−1.4114	−6.5992	−23.8804
12.00	−10.8954	0.0385	−0.7719	3.9761	−10.8263	−1.5675	−6.7605	−24.3082
13.00	−11.4600	−0.3599	−1.1369	3.6830	−10.8944	−1.5697	−6.7559	−24.6951
14.00	−11.8237	−0.4318	−1.4669	3.4849	−11.1165	−1.5781	−7.0757	−25.0005
15.00	−12.3468	−0.5425	−2.0405	3.1756	−11.3386	−1.5866	−7.1324	−25.3554
20.00	−14.1608	−1.5253	−3.6881	2.1754	−12.1087	−2.0521	−7.6406	−26.8045
25.00	−15.1616	−2.0191	−5.1670	1.5114	−13.2160	−2.5176	−8.0062	−27.4664
30.00	−16.4635	−2.5109	−6.3955	1.0297	−14.0069	−2.6949	−8.3286	−28.0888

REFERENCES

[1] Z. Gholamzadeh, S.M. Mirvakili, H. Khalafi, Neutronics investigation of CANADA Deuterium Uranium 6 reactor fueled (transuranic-Th) O_2 using a computational method, Nucl. Eng. Technol 47 (2015) 85–93.
[2] Atomic Energy of Canada Limited, ACR-700 Technical Description, 10801-01371-TED-001, 2003.
[3] J.H. Bae, J.Y. Jeong, Thermal–hydraulic characteristics for CANFLEX fuel channel using burnable poison in CANDU reactor, Nucl. Eng. Technol 47 (2015) 559–566.
[4] J.J. Whitlock, W.J. Garland, M.S. Milgram, Effects contributing to positive coolant void reactivity in CANDU, Trans. Am. Nucl. Soc 72 (1995) 329–330.
[5] C.A. Cotton, D. Lee, T.J. Downar, Coolant void reactivity analysis of CANDU and ACR-700 lattices, Trans. Am. Nucl. Soc 90 (2004) 587–589.
[6] C.A. Cotton, D. Lee, T. Kozlowski, T.J. Downar, W.S. Yang, D.E. Carlson, Physics analysis of coolant voiding in the ACR-700 lattice, Trans. Am. Nucl. Soc 92 (2005) 685–687.
[7] MCNP6 User's Manual, LA-CP-13-000634, version 1.0, Los Alamos National Laboratory Report, 2013.
[8] L.L. Carter, R.A. Schwarz, The visual creation and display of MCNP geometries and lattices for criticality problems, Trans. Am. Nucl. Soc 80 (1999). CONF-990605.
[9] J. Choe, H.C. Shin, D. Lee, New burnable absorber for long-cycle low boron operation of PWRs, Ann. Nucl. Energy 88 (2016) 272–279.